Microsyst Technol (2015) 21:1595–1605
DOI 10.1007/s00542-014-2376-4

TECHNICAL PAPER

Aspects of cavity filling with nano imprint

Hella-C. Scheer · M. Papenheim · K. Dhima · S. Wang · C. Steinberg

Received: 26 May 2014 / Accepted: 17 November 2014 / Published online: 31 December 2014

Abstract The role of capillary forces with nanoimprint is addressed. As the respective capillaries are the closed cavities of the stamp used for replication, the Laplace pressure together with the pressure of the gas phase inside the cavities dictate the equilibrium pressure in the polymer. Whether the cavities can be successfully filled, depends on the external pressure available from the imprint system, setting the pressure in the polymer, and on the sorption of any gaseous phase. Gas sorption is provided by the imprint polymer itself and may differ with different imprint materials and different imprint situations (imprint temperature, residual layer thickness). With soft stamps or composite stamps also the stamp itself may contribute to the overall gas sorption. Situations typical of different imprint techniques (thermal nanoimprint, UV-assisted nanoimprint, capillary force lithography) as well as of moulding during stamp replication are discussed in view of capillary effects. The discussion is illustrated by simple analytical estimations.

1 Introduction

Nanoimprint relies on the replication of the structures of a master into a thin polymeric layer on a hard substrate. When used as a lithography technique [nanoimprint lithography (NIL) (Chou et al. 1996; Guo 2004; Schift 2008)] any residual layer remaining below the elevated patterns of the stamp should be thin and, in particular, highly uniform; its removal is often provided by dry etching, and any over-etching necessary due to the non-uniformity of the residual layer may reduce the lateral dimensions of the structures.

Often the master itself is used as the stamp in the imprint process; with T-NIL (thermal NIL) Si and SiO_2-on-Si stamps are most prominent (Park et al. 2004; Zhao et al. 2008), with UV-NIL (UV-assisted NIL) quartz stamps are widely used (Hess et al. 2004). Also replica stamps are of growing interest to reduce the overall costs of the process, so as, e.g., Ni shims (Hirai et al. 2002) replicated by means of galvanics and polymer-based replica prepared by the moulding of the master with an Ormocer (Mühlberger et al. 2009; Schift et al. 2009), a PUA (polyurethaneacrylat) (Choi et al. 2004; Choi et al. 2011) or PDMS (polydimethylesiloxane) (Kim et al. 2001), often provided with a backplane of thin glass (Schmid and Michel 2000; Odom et al. 2002; van Delft et al. 2010). With such composite stamps the thickness of the polymeric layer is in the range of 10 µm up to some millimeters. The stamps (masters and replica) may be classified as hard stamps (Si, SiO_2, Ni) or soft (composite) stamps (Ormocer, PUA, PDMS). This differentiation is of practical importance for the nanoimprint process. Compared to hard stamps (Scheer et al. 2009), soft stamps provide a limited mechanical stability when elevated pressures are involved; but in contrast to hard stamps, soft stamps are able to absorb gases to some extent. This ability is characterised by the temperature dependent sorption coefficient. With hard stamps gas sorption is provided by the imprinted material primarily. PDMS replica without backplane are used in capillary force lithography (CFL) (Suh and Lee 2002a), where the stamp is laid on the polymeric layer (containing residual solvent) at a somewhat elevated temperature without any external pressure applied; the assembly is left for a sufficient time, often for hours and days, in order to allow the polymer to fill the stamp cavities by capillary forces.

H.-C. Scheer (✉) · M. Papenheim · K. Dhima · S. Wang · C. Steinberg
Microstructure Engineering, Department E: Electrical, Information and Media Engineering, University of Wuppertal, Rainer-Gruenther-Str. 21, 42119 Wuppertal, Germany
e-mail: scheer@uni-wuppertal.de

Typically, with T-NIL high temperatures (well above the glass transition temperature of the polymer in use) as well as high pressures (10–100 bar) are involved (Chou et al. 1996; Scheer and Schulz 2001; Schift 2008). With UV-NIL the imprint at room temperature and at reduced pressure is most typical (Vratzov et al. 2003). Hybrid systems also provide elevated pressure and elevated temperature in addition to UV exposure (Kim et al. 2008). Some systems provide an evacuation of the gap (Roos et al. 2003) between stamp and sample before imprint. Alternatively, gas condensation has been proposed to improve cavity filling (Hiroshima and Komuro 2007).

Stamp replication by moulding and CFL both have to rely on capillary effects in order to fill the cavities of the stamps. With T-NIL, due to the high pressure available, capillary effects are of minor relevance; nonetheless they may contribute to filling when small stamp cavities are involved. UV-NIL is in between; capillary effects are most important when liquid resists are used.

This contribution addresses the question of how far cavity filling proceeds when capillary forces are involved. The question is discussed in context with several typical situations during T-NIL, UV-NIL, CFL and stamp replication by moulding. The situations are analysed by simple analytical calculations considering gas sorption within the polymeric components involved.

2 Capillaries with nanoimprint

With nanoimprint, the capillaries involved are the trenches within the stamp. These trenches may be linear ones (long lines) or more dot-like ones (holes). In contrast to most capillary-related phenomena the capillaries with nanoimprint are closed ones (Scheer et al. 2013). Accordingly, when the capillary fills any gas contained in the trench volume initially has to become compressed and may enter the surrounding material by sorption. With capillaries, the pressure difference between the gas phase and the liquid phase is the well-known Laplace pressure (Landau and Lifschitz 2007); its size is defined by the two-dimensional curvature of the interface, κ, and the surface tension of the liquid, the polymer, γ_{pol}, in contact to the capillary wall, the stamp.

When an equilibrium is reached, the interface has adopted a minimum area representing a spherical or cylindrical cap (Suh et al. 2004). Then the curvature, κ, is simply related to the respective geometry of the cavity, b, and the Laplace pressure Δp_{La} amounts to

$$\Delta p_{La} = p_g - p_{pol} = \gamma_{pol} \cdot \kappa = \gamma_{pol} \cdot f \cdot \frac{cos\theta_0}{b} \qquad (1)$$

with θ_0 the equilibrium contact angle between the stamp and the polymer, and f a factor. f and b amount to 1 and $w/2$ (the half-width of the cavity) in case of a long, linear cavity and to 2 and r (the cavity radius or cavity half-width) in case of a dot-like, circular or square cavity. Thus, the Laplace pressure differs by a factor of two only in these extreme cases, with rectangular cavities lying in between.

The equilibrium contact angle is not an independent parameter but depends on the materials in contact, the stamp and the polymer. Assuming the simplest relationships, the Young equation (Young 1805; Good 1992) describing the equilibrium contact angle cos θ_0 as a function of γ_{pol} and the surface energy of the stamp, γ_{stamp}, where the interface energy is defined as the geometric mean (Good 1992) of the two materials in contact, the Laplace pressure can be expressed by the respective material constants according to

$$\Delta p_{La} = \frac{f}{b} \cdot \gamma_{pol} \left(2\sqrt{\frac{\gamma_{stamp}}{\gamma_{pol}}} - 1 \right). \qquad (2)$$

Curves for the contact angle and the Laplace pressure as a function of the surface tension of the polymer in contact to a stamp of different surface energy are given in Fig. 1. With values $\gamma_{pol} \leq \gamma_{stamp}$ the spreading regime (*) is entered, with the contact angle equal to zero (complete wetting) and maximum values of the Laplace pressure. Only with values $\gamma_{pol} > \gamma_{stamp}$ a contact angle $\theta_0 > 0$ develops and the Laplace pressure decreases. At values $\gamma_{pol} \geq 4\gamma_{stamp}$ the magic boundary ($\theta_0 = 90°$) is crossed and the Laplace pressure changes its sign, going from positive to negative values (only positive values are shown in Fig. 1b). Negative Laplace pressures are problematic as they counteract a self-filling of the cavities without an external pressure applied.

The calculation of the Laplace pressure in Fig. 1b is based on a linear cavity of half-width $b = w/2 = 100$ nm. Assuming cavities of 10 nm half-width as the smallest ones, realistic Laplace pressures in an imprint situation may be ten times higher than the values shown in Fig. 1b. [A lower boundary (about 10 nm) for the capillaries discussed here is suggested, as molecular size effects (Taga et al. 2010) and, e.g., thin-film induced mobility changes (Roth and Dutcher 2005) are not considered with the continuum-equations used].

Most relevant regimes in the context of nanoimprint are marked in Fig. 1. With an anti-sticking layer (ASL) on a stamp the surface energy typically varies from around 10 mN/m for an excellent ASL up to values of about 20 mN/m for a still useful ASL (Schift et al. 2005; Scheer et al. 2008). The polymer surface tensions feature similar values in the range of around 30–40 mN/m with T-NIL and UV-NIL as well, T-NIL tending towards lower values during the process due to the increased processing temperature. Equilibrium contact angles are in the range of $60° \leq \theta_0 \leq 85°$ and $65° \leq \theta_0 \leq 90°$, respectively. Such

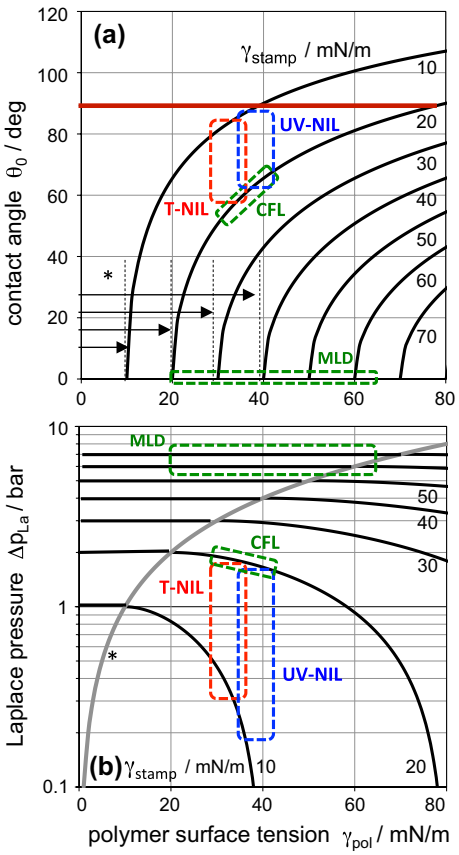

Fig. 1 Equilibrium contact angle (**a**) and Laplace pressure (**b**) as a function of the surface tension of the polymer or resist used, γ_{pol}. The curves refer to different surface energies of the stamp, γ_{stamp}, the cavity half-width b is assumed to 100 nm. The *arrows* in (**a**) as well as the grey line in (**b**) (both marked by *asterisk* indicate the spreading regime ($\theta_0 = 0$) and its boundary. Regimes for typical imprint situations are marked: T-NIL: γ_{pol} 30-35 mN/m (elevated temperature); γ_{stamp} 10–20 mN/m, according to ASL used. UV-NIL: γ_{pol} 35–40 mN/m (room temperature); γ_{stamp} 10–20 mN/m, according to ASL used. CFL: γ_{pol} 30–40 mN/m (depending on process temperature); γ_{stamp} ≈20 mN/m, according to PDMS. MLD (molding): γ_{pol} 20 mN/m (PDMS); γ_{stamp} 30–40 mN/m (polymer stamp) or 60–70 mN/m (stamp from Si or SiO_2/Si). For moulding with higher surface tension materials (Ormocer, PUA) and with masters featuring an ASL see text

values have also been observed experimentally (Bogdanski et al. 2008). With CFL the surface energy of the stamp (PDMS) has a fixed value, about 20 mN/m, decreasing with increasing temperature. Polymer surface tensions are similar to the ones with T-NIL and UV-NIL, resulting in contact angles of $50° \leq \theta_0 \leq 70°$ (Suh and Lee 2002b, 2004). With PDMS-moulding (MLD) often no anti-sticking layers are used, in particular when a photoresist pattern is replicated. In this case a typical surface energy of the stamp is about 40 mN/m with a polymeric pattern and 60–70 mN/m with a Si/SiO_2 pattern of the template. With a surface tension of ≈20 mN/m molding with PDMS proceeds in the spreading regime.

With respect to capillary filling Fig. 1 already indicates typical issues. Moulding with PDMS in the spreading regime can safely rely on high Laplace pressures for cavity filling. When, in order to improve separation after moulding, the surface of the template is provided with an ASL [this may be required when undercut structures are involved (Möllenbeck et al. 2007)], the situation becomes less beneficial, as the contact angle increases ($\theta_0 \approx 60°$) and the Laplace pressure decreases accordingly. When moulding with higher surface tension materials (Ormocer 41 mN/m, Finn et al. 2013 and PUA 35 mN/m, Choi et al. 2011) spreading will still prevail in case of higher-energy masters like Si or SiO_2, without an ASL. However, successful separation after moulding asks for an ASL. Then, with an ASL of good quality (≈10 mN/m), the contact angle is near 90° and only small Laplace pressures prevail; even negative Laplace pressures are conceivable under unfavourable conditions. Thus, moulding with an Ormocer or PUA may be problematic. The strategy followed to formulate such materials with a fluorine (Tsunozaki and Kawaguchi 2009) or siloxane additive or component (Choi et al. 2004; Yoo et al. 2004) lowering the surface tension suggests an improvement not only of separation but also of filling. Surface energies as low as ≈ 20 mN/m are reported for such materials (Choi et al. 2011; Finn et al. 2013).

CFL, due to its beneficial surface energy of ≈20 mN/m can benefit from still relatively high Laplace pressures for cavity filing, almost independent of the moulding material used. T-NIL und UV-NIL work in a range of moderate Laplace pressures. With UV-NIL the Laplace pressure tends to be even lower than with T-NIL, due to room temperature processing. The better the ASL of the stamps used the lower the Laplace pressure; thus UV-NIL with excellent ASLs turns out to be problematic; very low surface energies of the stamp may even induce negative Laplace pressures that counteract filling.

3 Gas sorption with imprint-relevant materials

Complete filling of a closed cavity is only possible when any gas contained in the stamp cavities, be it at atmospheric pressure or below atmospheric pressure, is absorbed by or dissolved in the material surrounding the enclosed gas, the polymeric material used for the imprint or the stamp (in case of a soft stamp or a composite stamp), or both. Physically, the gas has to diffuse into the adjacent material. In case of CFL it will not only diffuse into the stamp but even through the stamp, which is particularly supported by applying an external vacuum during CFL. Most critical are situations where the amount of material able to absorb any gas is comparably small; this is the case with hard stamps, in particular when also the volume of the imprint polymer is reduced to

Table 1 Data used for the estimation of the sorption of gas within the imprint polymer and the stamp, together with its temperature dependence

		S(298 °C)/bar^{-1}	$\Delta E/R$/K	References
polymer > T_g	N_2	0.054	$+0.29 \cdot 10^3$	van Krevelen (1990)
	O_2	0.117	$-0.07 \cdot 10^3$	
polymer < T_g	N_2	0.02	$-0.21 \cdot 10^3$	van Krevelen (1990)
	O_2	0.047	$-0.57 \cdot 10^3$	
PDMS	N_2	0.09*	$+0.8 \cdot 10^3$**	*Merkel et al. (2000); **van Krevelen (1990)
	O_2	0.18*	$-0.5 \cdot 10^3$**	

Generally, data for imprint polymers above T_g are used with T-NIL, data for polymers below T_g are used with UV-NIL

get low or negligible residual layers. The worst case situation discussed in paragraph 4 will be the one with zero residual layer, where all initial gaseous filling of a cavity has to be contained in the polymer when the cavities are filled.

For a diffusion-based process the primary material parameter is the diffusion constant D, the material constant within the differential equation describing a diffusion process. Together with the concentration gradient it defines any particle transport through a material (diffusion current). Typically, concentrations c representing a solution to the diffusion equation feature an argument combining time- and space- behaviour, $c(x/2\sqrt{Dt})$ (Crank 1975).

Additionally, in case of gas sorption, further material parameters (Crank 1975; van Krevelen 1990; Merkel et al. 2000) are the sorption constant S and the permeability constant P. The quantity S in units [cm^3(STP)/(cm^3 bar)] gives the volume of gas under standard conditions [standard pressure and temperature (STP)] that can be absorbed in a polymeric material or a membrane per volume at a partial pressure p of, e.g., 1 bar. The permeation coefficient P in units [cm^3(STP)/(s·bar) × cm/cm^2] gives the volume of gas (STP) passing per time and area across a membrane of a certain thickness at a certain pressure difference.

In the case of 'simple' gases, where no specific interaction with the polymer/membrane occurs, the diffusion constant remains constant [$D \neq D(c)$] and the following relationships are valid (van Krevelen 1990; Sperling 2001) as long as the pressure is not too high:

$$P = D \cdot S, \quad c = S \cdot p, \tag{3}$$

the second relationship representing Henrys' law with p the partial pressure in case of a gas mixture. Thus, the permeation constant is linearly related to the sorption constant. As diffusion constants for simple gases in polymeric materials are almost similar ($D \approx 10^5 cm^2/s$, van Krevelen 1990), the behaviour is governed by the sorption constant S. Similarly, the concentration c of a gas in the polymer/membrane is linearly proportional to the sorption constant S; the higher the partial pressure p of the respective gas the higher the concentration achievable. This is understandable in view of a material offering some empty space (the free volume of a polymer). The free volume provides a continuous connection through the whole polymer, although with a limited permeability (like a membrane); this free volume can be filled with compressed simple gases; when both surfaces are open the gas can pass through or be pumped through the polymer. This simple picture also allows to understand that polymers used above their glass transition temperature, T_g, due to their higher free volume and higher segmental mobility, provide a higher sorption for gases than polymers used below their T_g. The temperature behaviour of all parameters, D, S and P, follows an Arrhenius relation [~exp(–$\Delta E/RT$)], with R the gas constant and positive and/or negative activation energies (ΔE) as well. The material parameters used in Sects. 4 and 5 are listed in Table 1. The values for air were calculated on the basis of a composition of 79 % N_2 and 21 % O_2, taking into account the respective partial pressures. (In order to hold the calculations simple Henrys' law is used throughout the calculations, although a nonlinear relationship might be more correct at high imprint pressure.)

For the calculations performed here only the sorption constant is required. Typical sorption data used in the next paragraphs are given in Fig. 2. Figure 2a shows the sorption of a typical polymer used for T-NIL as a function of temperature. The sorption for O_2 is higher than for N_2, with differing temperature dependence. The resulting sorption for air amounts to 7–9 % at 1 bar, depending on the temperature. Figure 2b compares typical situations with nanoimprint. With T-NIL, polymers are processed above their T_g, featuring medium values of air sorption ($S \approx 8$ % bar^{-1} at 170 °C). With UV-NIL operating at room temperature sorption may be smaller ($S \approx$ 2–3 % bar^{-1} for a polymer below its T_g, see van Krevelen 1990). Sorption data for specific UV-NIL materials are not at hand. We assume maximum values similar to those of a polymer at room temperature, ≈6 %bar^{-1} at most, lower than with T-NIL. The high sorption reported for PDMS ($S \approx$ 10–25 % bar^{-1}, Merkel et al. 2000) represents a specific characteristic of this elastomeric material often made use of. Gas permeation through the PDMS (P being high due to the high sorption S, Eq. 3) will not be considered here. Therefore, the calculations for PDMS rather document a 'worst case' situation.

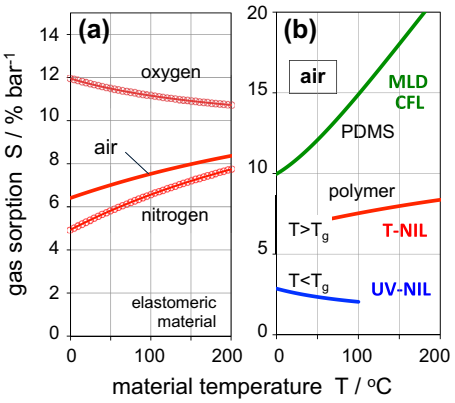

Fig. 2 Sorption data and their temperature dependence according to Table 1. **a** Sorption for air (79 % N_2, 21 % O_2) as calculated from the sorption for N_2 and O_2 in case of a polymer used above its T_g, in the elastomeric range. **b** Sorption data used for UV-NIL (polymer below T_g or resist/liquid at low sorption), T-NIL (polymer above T_g) and CFL and moulding (PDMS)

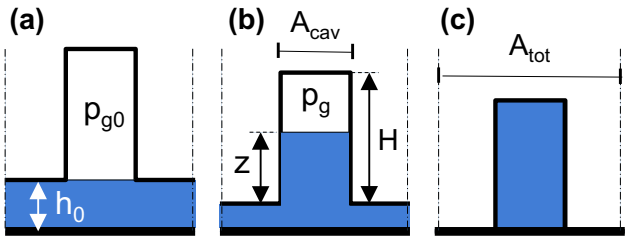

Fig. 3 Geometry used for the estimation of cavity filling under worst-case conditions (hard stamp, minimum polymer volume available for sorption); section of a periodic cavity sequence (sketch without Laplace pressure, areas A_{cav} and A_{tot} shown in projection, only). **a** Initial: the cavities (height H, area A_{cav}) are filled with air at some pressure p_{g0}. The polymer available is adequate to fill the cavity. **b** Partial filling: the cavities are filled with polymer up to a height z; the gas pressure is increased $p_g > p_{g0}$. **c** Total filling: the cavities are completely filled with polymer and no residual layer remains

4 Impact of gas sorption

With data for the sorption of air on hand the filling of cavities can be estimated by simple analytical calculations. Cavities of the same size and a height H are assumed in the stamp. For a worst case calculation (see Fig. 3) the stamp is assumed to be rigid, and the polymer material available per area is assumed to be sufficient to fill the stamp cavities, without any residual layer remaining ($V_{pol} = h_0 A_{tot} = H \cdot A_{cav} = V_{cav}$). Thus, under these worst-case conditions, all the air residing in the cavities at the beginning of the imprint (Fig. 3a) has to become absorbed in a polymer volume equal to the cavity volume (Fig. 3c). (Any air gap due to non-conformal contact between stamp and sample surface is neglected.) Furthermore, the gas is assumed to behave like an ideal gas (no transition to a liquid state), following the relationship $pV/T = \text{const}$.

First the situation without Laplace pressure ($\Delta p_{La} = 0$) and without sorption ($S = 0$) is investigated. Under these conditions, when the stamp cavity is filled up to a height z (Fig. 3b), the gas phase becomes compressed and the gas pressure p_g is given by

$$p_g = p_{g0} \cdot \frac{T}{T_0} \cdot \frac{V_0}{V} = P_{g0} \cdot \frac{T}{T_0} \cdot \frac{H}{H - z} = p_{g0} \cdot \frac{T}{T_0} \cdot \frac{1}{1 - \left(\frac{z}{H}\right)}. \quad (4)$$

Here p_{g0}, V_0 and T_0 refer to the initial situation, the initial gas pressure (atmospheric pressure or below), the initial temperature where stamp and sample are brought into contact, and the initial volume available for the gas phase $V_0 = V_{cav} = A_{cav} H$, with H the total height of the cavity. T is the imprint temperature and V is the volume available for the gas in an intermediate filling situation (Fig. 3b), $V = A_{cav}(H - z)$, with z the filling level counted from the stamp surface. As shown in Eq. (4), the resulting pressure in the gas phase is a function of one single parameter, the relative amount of filling of the cavitiy, z/H.

This equation can be modified quite simply to account for gas sorption. With a sorption $S > 0$ the initial volume of the gas phase is $V_0 = V_{cav} + S \cdot V_{pol} = A_{cav} H(1 + S)$—the gas not only fills the cavity but some amount of it is already absorbed in the polymer before stamp contact; at some filling level then the volume available for the gas amounts to $V = A_{cav}(H - z) + S \cdot V_{pol} = A_{cav}(H(1 + S) - z)$. If, in addition, it is assumed that more polymer is available than simply the one required to fill the cavity, say $V_{pol} = a \cdot V_{cav}$, then this further factor a (relating the polymer volume available per cavity to the cavity volume itself) enters the correlation, additionally. Equation (4), modified to account for gas sorption and polymer availability, then reads:

$$p_g = p_{g0} \cdot \frac{T}{T_0} \cdot \frac{H \cdot aS}{H \cdot aS - z} = P_{g0} \cdot \frac{T}{T_0} \cdot \frac{1}{1 - \left(\frac{z}{H}\right) \cdot \left(\frac{1}{aS+1}\right)} \quad (5)$$

with S the sorption constant and a the relative availability of polymer, $a = V_{pol}/V_{cav}$. The factor a may comprise not only the imprint polymer available, when the imprint is performed with a certain residual layer; it may also comprise the additional polymer volume in a soft stamp that is able to absorb gas. In case the imprint polymer and the soft stamp have different sorption values the term $(a \cdot S)$ in Eq. (5) can be replaced by $(a_{pol} S_{pol} + a_{stamp} S_{stamp})$ to account for this situation. As indicated in Eq. (5), there are now two parameters defining the pressure in the gas phase, z/H and $a \cdot S$, the total sorption.

So far only the pressure in the gas phase has been accounted for. Now, in a second step, the cavity has to be considered as a closed capillary; then, depending on the contact angle, a certain curvature of the interface develops. This curvature is related to a positive (or negative) Laplace pressure Δp_{La} across the interface. Thus, the pressure in the

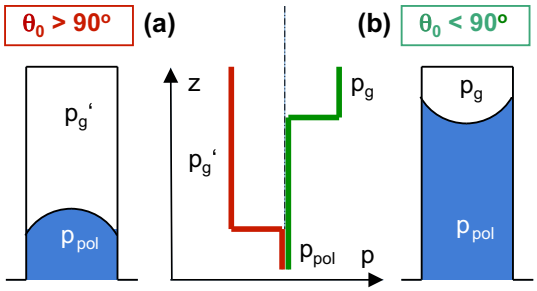

Fig. 4 Situations with partly filled closed cavities, assuming a similar pressure in the polymer. **a** When the contact angle is above 90° (negative Laplace pressure), the pressure in the gas phase is lower than in the polymer. **b** When the contact angle is below 90° (positive Laplace pressure), the pressure in the gas phase is higher than the pressure in the polymer

liquid, the polymer, can be estimated from the pressure in the gas phase according to

$$p_{pol} = p_g\left(\frac{z}{H}, a \cdot S\right) - \Delta p_{La} \tag{6}$$

with Δp_{La} given by Eq. (2). Equation (6) gives the pressure in the polymer when an equilibrium, steady-state situation with a certain filling level z is reached. Without gravity and without flow the pressure in the polymer is constant. The pressure in the polymer is the pressure that has to be provided by the imprint system.

Figure 4 depicts the situation of a partly filled cavity at a similar pressure in the polymer, with a negative (Fig. 4a) and a positive (Fig. 4b) Laplace pressure of similar size denoting the pressure difference between polymer and gas at the meniscus. (—the initial situation was dissimilar; the cavity might have been evacuated initially in case of Fig. 4a but was at atmospheric pressure in case of Fig. 4b). With a positive Laplace pressure the pressure in the polymer is lower than in the gas phase, and the gas is easily compressed; the positive Laplace pressure aids to fill the cavities. With a negative Laplace pressure the pressure in the polymer is higher than the pressure in the gas phase; the filling of the capillary is hampered and requires an increased pressure in the polymer.

Figure 5 shows the equilibrium pressure in the imprint polymer as a function of the relative amount of cavity filling, z/H. The worst-case situation is calculated, imprint with a hard stamp, minimum polymer volume available ($a = 1$) and no pre-evacuation ($p_{g0} = 1$ bar). Curves for different values of the Laplace pressure are given; maximum values of (positive) Laplace pressure in a typical imprint situation amount to about 30 bar (dot-like cavity, 10 nm radius, compare Fig. 1b). Figure 5a refers to a situation without sorption, $S = 0$. Without Laplace pressure ($\Delta p_{La} = 0$), a 50 % filling requires a pressure of 2 bar, as expected. With a Laplace pressure of +1 bar this filling

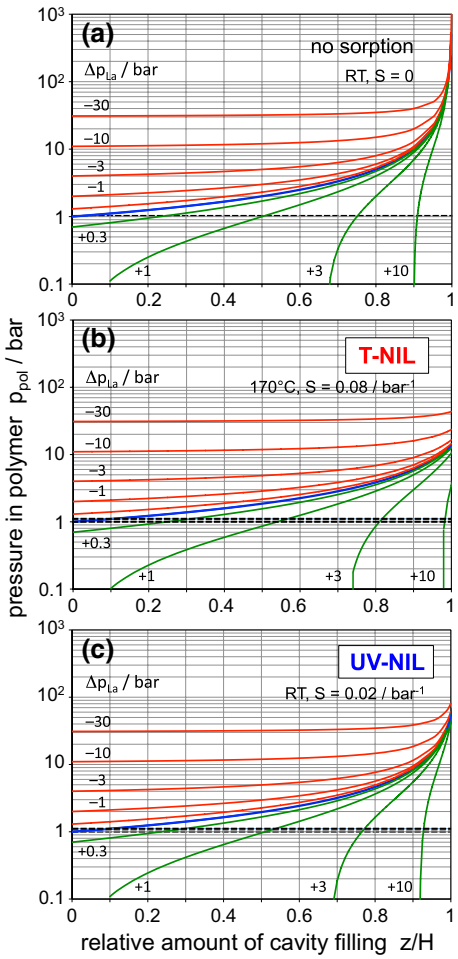

Fig. 5 Pressure in the imprint polymer under equilibrium conditions as a function of the relative amount of filling of the cavities, z/H. Calculation under worst-case conditions (hard stamp, $a = 1$, cavity initially under atmospheric pressure). The parameter Laplace pressure is varied according to a logarithmic scale, $\pm\Delta p_{La} = (0.3, 1, 3, 10, 30)$ *bar*, as indicated. Atmospheric pressure is marked by the dashed line. **a** Without sorption ($S = 0$), calculation for room temperature. **b** With moderate sorption ($S = 0.08$ bar^{-1}), calculation for 170 °C. **c** With low sorption ($S = 0.02$ bar^{-1}), calculation for room temperature

level is already obtained with a pressure of 1 bar, as the Laplace pressure acts similar to an external pressure. With a Laplace pressure of 10 bar, the cavities become self-filled by 90 %. Any further filling will require external pressure (pressure in the polymer beyond atmospheric pressure) which has to be provided by the imprint system. With negative Laplace pressures any filling of the cavities requires external pressure, as at least the Laplace pressure has to be overcome to hold the gas in the cavity. (When the pressure in the polymer is below atmospheric pressure, there is capillary suction between the stamp and the sample.)

For all values of the Laplace pressure the curves of Fig. 5a coincide and tend towards infinity for high z/H. A complete filling (100 %) is not possible without air

sorption; this has to be expected from Eq. (4) as with $z = H$ the denominator becomes zero. This is different when sorption is considered as shown in Fig. 5b. The curves refer to a typical situation in T-NIL; an imprint temperature of 170 °C is assumed (typical of the imprint of PS) and a sorption of $S = 0.08$ bar^{-1}, in accordance with Fig. 2. Now a complete filling of the cavities is possible with a finite value of pressure. Without the help of Laplace pressure 20 bar are sufficient to fill the cavities; with a positive Laplace pressure the pressure required will be reduced to about 10 bar; even with a negative Laplace pressure of up to −30 bar complete cavity filing is obtained at pressures of 50 bar. As pressures of 20–100 bar are quite typical of T-NIL (Scheer et al. 2005), any cavity can be filled, largely independent of the situation (polymer and stamp surface energy). Aiding or hindering by a positive or negative Laplace pressure is an issue with cavities of small geometry only; larger cavities (>100 nm in width) of any geometry are well characterized by $\Delta p_{La} = 0$ (see Fig. 1b). With a residual layer remaining ($a > 1$) the situation will be even more relaxed.

Figure 5c shows a situation with a low sorption level ($S = 0.02$ bar^{-1}) as might be typical of UV-NIL with a hard stamp at room temperature. Again the cavities are filled with air under atmospheric pressure, initially. Complete filling of the cavities is not possible without any external pressure, even at high values of the Laplace pressure—this was already expected from the results shown in Fig. 5a. Even under favourable conditions (high positive Δp_{La}) a pressure of 50–60 bar is required for complete cavity filling; with negative values of Δp_{La} a high pressure is already required to fill the cavities to some extent. With limited external pressure provided by the imprint system UV-NIL has to rely on positive Laplace pressures. Small cavities (high Laplace pressure) are easier to fill than large ones (zero Laplace pressure). At similar pressure in the polymer the filling level obtainable with small cavities is higher than with large cavities. Thus, availability of pressure in a UV-NIL imprint system is a crucial issue. The only means to improve the situation is to provide a much larger volume of polymer that can absorb the air, either by imprinting with a high residual layer (or a thick transfer layer or planarization layer below the imprint polymer, Xu et al. 2004) in case of a hard stamp, or by using a soft stamp that can absorb air efficiently. Furthermore, pre-evacuation of the gap between stamp and substrate will relax the situation.

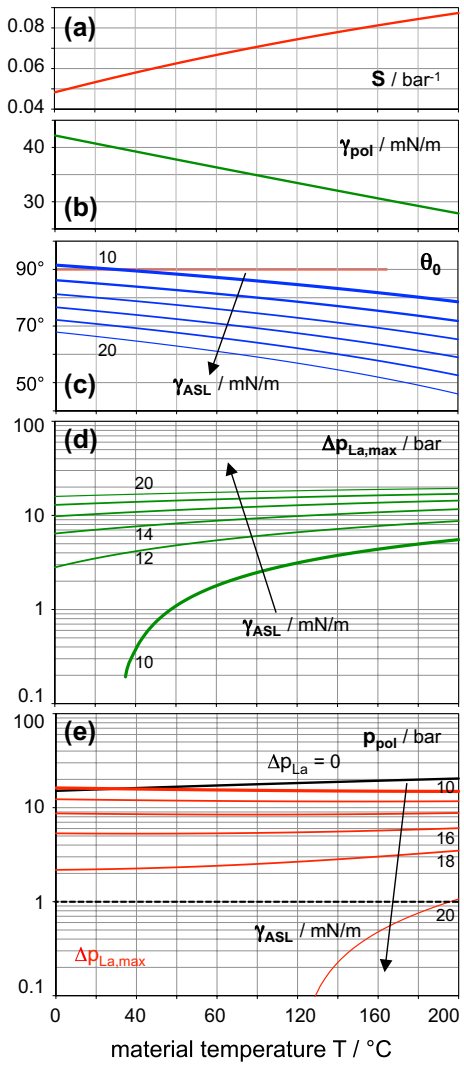

Fig. 6 Temperature behaviour of properties relevant for cavity filling. (Ordinate labelling is provided by formula symbols within the single figures.) **a** Sorption of air (S), assuming data for a polymer above its T_g (Table 1, first 2 lines). **b** Surface tension of polymer (γ_{pol}) used for imprint (example PS), temperature dependence according to Guggenheim-relationship. **c** Equilibrium contact angle (θ_0) developing between the imprint polymer and the mould, covered with an anti-sticking layer (ASL). The surface energy of the ASL, γ_{ASL}, is varied from 10 mN/m to 20mN/m in steps of 2 mN/m. **d** Maximum Laplace pressure ($\Delta p_{La,max}$) calculated for a linear cavity of 10 nm half-width. γ_{ASL} similar to c). **e** Pressure in the polymer (p_{pol}) required to completely fill the cavities ($z/H = 1$) under worst-case conditions (hard stamp, $a = 1$, no pre-evacuation). *Black curve*: $\Delta p_{La} = 0$, referring to wide cavities. *Red curves* referring to maximum Laplace pressures $\Delta p_{La,\,max}$ as shown in d) as valid for small cavities. γ_{ASL} similar to c)

5 Temperature and quality of ASL

Figure 6 summarizes the temperature dependence of all parameters involved. As the data set available is most reliable for a polymer typical of T-NIL, the data for a medium value of sorption with a positive temperature dependence are used (first 2 lines of Table 1), together with a surface tension value corresponding to PS. The curves are given over a temperature range of 0–200 °C. Thus, not only the T-NIL situation is covered, but important aspects of room temperature (RT) processing with UV-NIL are included. Though different, the surface tension of materials used for

T-NIL and UV-NIL is in the same range, and the temperature dependence is quite similar. Thus, with respect to sorption a relaxed situation (highest S) is assumed for UV-NIL with a hard stamp, here.

Figure 6a gives the sorption for air. At RT it amounts to about 0.055 bar^{-1}, a value about twice as large as the value taken on the basis of available data (Table 1) for the calculations in Fig. 5c, but still lower than the data used for T-NIL in Fig. 5b. The temperature dependence corresponds to an Arrhenius-type behaviour according to the parameters listed in Table 1.

Figure 6b shows the surface tension of PS as an example, according to the relationship given by Guggenheim (van Krevelen 1990),

$$\gamma_{pol} = \gamma_{pol,0} \cdot \left(1 - \frac{T}{T_c}\right)^{11/9}, \tag{7}$$

with values $\gamma_{pol,0}$ and T_c for PS amounting to 63.3 mN/m and 967 K, respectively (van Krevelen 1990). Whereas the surface tension is around 40 mN/m at RT, it amounts to about 30 mN/m at temperatures typical of T-NIL. This decrease results in a decrease of the equilibrium contact angle θ_0 and a corresponding increase of the Laplace pressure Δp_{La} (see Fig. 6c, d). The surface energy of the stamp is dictated by the ASL on its surface. To account for the quality of the ASL (and potential aging effects) values of γ_{ASL} between 10 mN/m (excellent quality) and 20 mN/m (low quality) are assumed (Scheer et al. 2008). Its temperature dependence is negligible in case of a hard stamp. [—Generally, the temperature dependence is primarily a consequence of thermal expansion effects (Israelachvili 2011)]. Figure 6c gives the equilibrium contact angle θ_0, assuming ASLs of 10–20 mN/m. With T-NIL, contact angles are $50° < \theta_0 < 80°$; with RT processing as typical of UV-NIL the contact angles are higher, where good ASLs increase the risk to cross the 90° borderline (red) and to enter the regime of negative Laplace pressures—this was already indicated in Fig. 1. Thus, for RT processing, an excellent ASL rather hampers cavity filling.

Figure 6d shows the maximum Laplace pressures corresponding to Fig. 6c, when assuming a cavity half-width of 10 nm. Thus, with cavities ranging from $w/2 = 10$ nm to micron sized cavities the Laplace pressure varies from $\Delta p_{La,max}$ to $\Delta p_{La} = 0$. With RT processing, the ASL quality severely affects the processing result as the Laplace pressure varies substantially with γ_{ASL}. With an ASL of 10 mN/m, Δp_{La} becomes negative for temperatures below about 30 °C, in accord with the crossing of the 90° boundary in Fig. 6c. Best filling (high Δp_{La}) goes along with high γ_{ASL},—in conflict with an easy separation of the replica from the stamp after processing. With T-NIL Δp_{La} is always positive and higher than with RT processing.

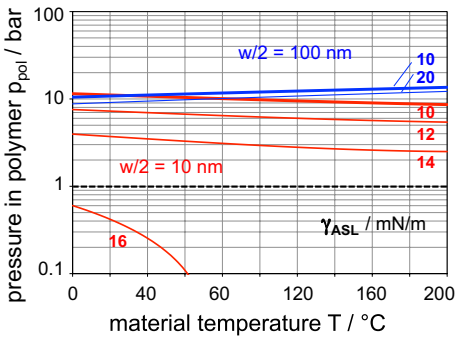

Fig. 7 Pressure in the polymer required for complete filling ($z/H = 1$) of single size cavities ($w/2 = 10$ nm and 100 nm) in a stamp with ASLs of the indicated surface energies γ_{ASL}. Sorption data similar to Fig. 6a, imprint with residual layer ($a = 1.5$)

Figure 6e finally shows the pressure in the polymer p_{pol} required for a complete filling of the cavities ($z/H = 1$) as calculated for the worst-case conditions (hard stamp, lowest polymer volume available for sorption ($a = 1$), no pre-evacuation). This pressure has to be provided by the imprint system used. The black curve refers to $\Delta p_{La} = 0$ and represents the situation with wide cavities, where filling is hardly aided by capillary effects. The curves in red refer to maximum values of the Laplace pressure as given in Fig. 6d; only positive Laplace pressures are considered. As already expected from Fig. 5d, the pressure required for complete cavity filing does not differ too much between situations with low positive Laplace pressure (red, $\gamma_{ASL} = 10$ mN/m) and zero Laplace pressure (black). The crossover between both curves corresponds to the transition to negative Laplace pressures at about 30 °C in Fig. 6d. Only with inadequate ASLs ($\gamma_{ASL} = 20$ mN/m) complete filling is obtainable at pressures only slightly exceeding 1 bar, at high temperature, a situation of hardly any practical impact. Again the results confirm that with a hard stamp and a low volume of polymer available for sorption of gas the imprint system has to provide external pressures beyond ≈10 bar in order to fill stamp cavities of differing size completely (black curve).

This is different when a stamp features one single cavity size, only. Then the Laplace pressure corresponding to this cavity size may be used for complete cavity filling under low external pressure. Figure 7 exemplarily shows this situation, referring to single-sized cavities of 10 nm and 100 nm half-width, respectively, in a hard stamp. In both cases an imprint with a residual layer is assumed ($a = 1.5$); the sorption data are similar to Fig. 6a. Due to the increased volume of polymer available for sorption, the pressure in the polymer now decreases with temperature at a high Laplace pressure (red curves). With single-sized cavities of 10 nm half-width and an ASL of medium quality (14–16 mN/m) a regime is met where almost atmospheric pressure

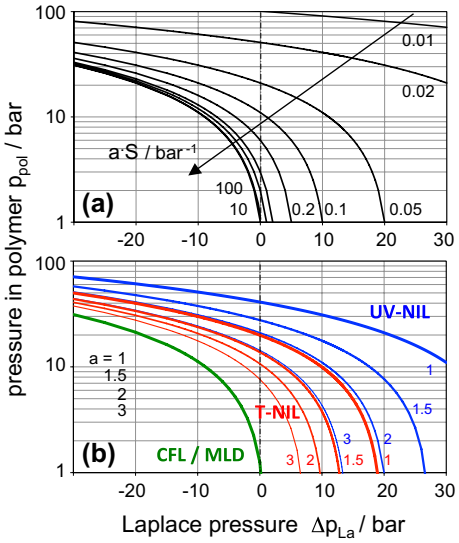

Fig. 8 Pressure in the polymer required for complete filling of the stamp cavities ($z/H = 1$) as a function of the Laplace pressure. The parameter varied is the total sorption $a{\cdot}S$. **a** General; parameter values shown: 0.01, 0.02, 0.05, 0.1, 0.2, 0.5, 1, 10, 100. **b** Range of UV-NIL ($S = 0.02$, $a = 1$, 1.5, 2, 3), T-NIL ($S = 0.08$, $a = 1$, 1.5, 2, 3) and CFL as well as moulding (MLD) ($S = 0.1$, $a = 100$–1,000)

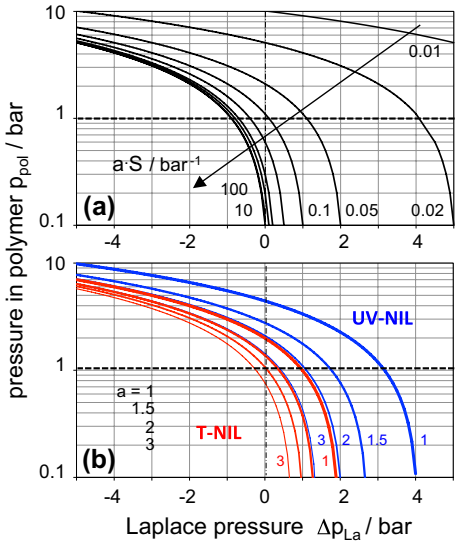

Fig. 9 Pressure in the polymer required for complete filling of the stamp cavities ($z/H = 1$) as a function of the Laplace pressure. The parameter varied is the total sorption $a{\cdot}S$. Pre-evacuation to 0.1 bar is assumed. **a** General; parameter values shown: 0.01, 0.02, 0.05, 0.1, 0.2, 0.5, 1, 10, 100. **b** Range of UV-NIL (S = 0.02, $a = 1$, 1.5, 2, 3) and T-NIL ($S = 0.08$, $a = 1$, 1.5, 2, 3)

is sufficient for cavity filling. This may be an interesting experimental regime, in particular for RT processing, when very small cavities are involved, only. With larger cavities (100 nm half-width) the effect of the Laplace pressure is already negligible and complete cavity filling requires at least 10 bar of external pressure, almost independent of the quality of the ASL (blue curves).

6 Total sorption and pre-evacuation

Complete filling of the cavities without pre-evacuation of the system highly depends not only on the gaseous sorption of the material involved (S) but also on the amount of material provided for sorption, as indicated in Eq. (5) by the factor a, the ratio of cavity volume to polymer volume available per cavity. Figure 8a gives the pressure in the polymer required for a complete filling of the cavities ($z/H = 1$) as a function of the Laplace-pressure for different values of $a{\cdot}S$ as a parameter, according to Eq. (5), without pre-evacuation. With high values of $a{\cdot}S$ in the range of 10–100 bar^{-1} a complete filling of the cavities is possible at almost atmospheric pressure even without the aid of a positive Laplace pressure. Such a situation exists in case of CFL or moulding, where ample polymeric material is involved to absorb any gaseous medium, as shown in Fig. 8b. As also indicated there, the situation with T-NIL and UV-NIL is less beneficial. Situations with differing polymer availability are shown; $a \geq 1.5$, e.g., characterizes residual layers of increasing thickness. With mixed cavities ($\Delta p_{La} = 0$) the pressure required for complete filling is reduced but stays in the range of 8–10 bar with T-NIL and 15–20 bar with UV-NIL. Only with very small cavities (high Δp_{La}) and thick residual layers ($a > 1.5$) the external pressure required for complete filling stays below 10 bar. In any case, the pressure available experimentally is set by the imprint system used and is thus limited.

When pre-evacuation of the gap between stamp and substrate is provided by the imprint system, the situation differs as shown in Fig. 9. It is assumed that during pre-evacuation not only the existing gap, but also the polymer has been evacuated; a pre-evacuation down to 0.1 bar is considered. Now the pressure range in the polymer is about a factor of 10 smaller than before, and the interesting regime of strong pressure change occurs within a much smaller range of Laplace pressures (Fig. 9a). This is the case as the Laplace-pressure is independent of the gas pressure but represents a pressure difference between gas phase and polymer, its value depending only on the materials in contact. (We suggest that any change of surface tension of the polymer is negligible within this pressure range). At a total sorption of only 0.02 a Laplace pressure of +4 bar is sufficient to fill the cavities completely at atmospheric pressure; with a total sorption of 0.1 the aid of Laplace pressure is not even required. Figure 9b indicates the situations typical with T-NIL and UV-NIL only, where pre-evacuation of the cavities in the hard stamp is of technical relevance. Figure 9b shows that now moderate residual layers ($a \approx 1.5$)

and small Laplace pressures are efficient to substantially reduce the external pressure required for complete cavity filling, in particular for not too low sorption values. As expected, pre-evacuation improves the situation substantially when hard stamps are involved in UV-NIL and T-NIL. Nonetheless, pre-evacuation asks for a more sophisticated imprint system and requires additional time, as the small gaps between stamp and substrate highly reduce the efficiency of pumping. Furthermore, liquid resists as sometimes used with UV-NIL preclude any evacuation.

7 Stamp material

As already shown in Fig. 8 the total sorption $a{\cdot}S$ is a good indicator of the characteristic situation of different imprint techniques. With hard stamps in T-NIL and UV-NIL, $a{\cdot}S$ is relatively low, increasing with processing temperature. In case of moulding the large volume of moulding material results in high values of $a{\cdot}S$. With CFL, the stamp material itself, PDMS, provides ample volume to absorb gaseous species, again resulting in high values of $a.S$. A similar effect should occur when T-NIL or UV-NIL are performed with a soft stamp (e.g., from Ormocer, PUA or PDMS) or with a composite stamp featuring, e.g., a glass backplane (Schift et al. 2009). Assuming a minimum thickness of the soft material in a composite stamp of about 10 µm and cavities of below 500 nm in height, a value of 20–100 may be estimated for the parameter a, depending on the geometries and the density of the cavities. Even with a moderate sorption of only 0.05 bar^{-1}, below the one of PDMS, values of $a{\cdot}S$ beyond 1 are obtained easily. Thus, with respect to sorption, soft stamps are of interest as they provide high total sorption, as indicated in Fig. 10, together with the typical situations for UV-NIL, T-NIL, CFL and moulding. The use of a soft stamp or composite stamp is of similar effect as a pre-evacuation and thus provides an interesting alternative to hold the imprint system simple and the process quick. However, the stability (Delamarche et al. 1997; Hui et al. 2002; Schift et al. 2009; Finn et al. 2013) with respect to mechanical and thermal loading and with respect to cleaning solvents may limit the use of soft stamps with nanoimprint despite their beneficial sorption property.

8 Summary and conclusion

Simple assumptions were made to illustrate the impact of capillary action on the filling of closed cavities in an imprint process and the role of the pressure in the polymer that has to be provided by the respective imprint system. Typical imprint situations with T-NIL, UV-NIL, CFL as well as moulding were addressed in the context with the

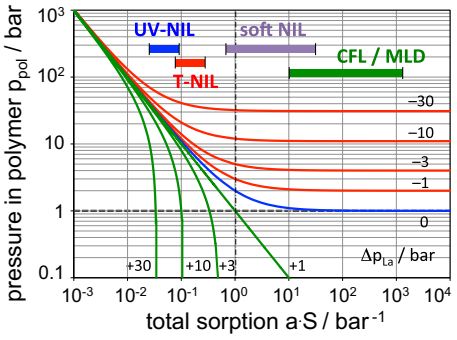

Fig. 10 Pressure in the polymer required for complete filling of the stamp cavities ($z/H = 1$) as a function of the total gas sorption $a{\cdot}S$. The green curves indicate the effect of a positive Laplace pressure; the red ones refer to a negative Laplace pressure. Typical regimes in terms of $a{\cdot}S$ for the different imprint techniques with soft stamps as well as hard stamps are indicated

property of the polymeric materials involved to absorb the gas initially contained in the cavities. Without pre-evacuation of the cavities a complete filling requires an imprint pressure in the range of 10 bar or more, unless a high volume of polymer is available to absorb the gas enclosed. The use of soft stamps or composite stamps has been shown to substantially relax the imprint situation.

It has to be emphasized that equilibrium conditions were calculated throughout, without considering any time dependence of cavity filling. Time dependence will be addressed in a forthcoming paper.

References

Bogdanski N, Moellenbeck S, Scheer H-C (2008) Contact angles in a thermal imprint process. J Vac Sci Technol B26:2416–2420

Choi S-J, Yoo PJ, Baek SJ, Kim TW, Lee HH (2004) An ultraviolet-curable mold for sub-100-nm lithography. J Am Chem Soc 126:7744–7745

Choi S-J, Kim HN, Bae WG, Suh K-Y (2011) Modulus- and surface energy-tunable ultraviolet-curable polyurethane-acrylate: properties and applications. J Mat Chem. doi:10.1039/c1jm12201k

Chou SY, Krauss PR, Renstrom PR (1996) Nanoimprint lithography. J Vac Sci Technol B 14:4129–4133

Crank J (1975) The mathematics of diffusion. Clarendon, Oxford

Delamarche E, Schmid H, Michel B, Biebuyck H (1997) Stability of molded polydimethylsiloxane microstructures. Adv Mater 9:741–746

Finn A, Lu B, Kirchner R, Thrun X, Richter K, Fischer W-J (2013) High aspect ratio pattern collapse of polymeric UV-nano-imprint mold due to cleaning. Microelectron Eng 110:112–118

Good RJ (1992) Contact angle, wetting and adhesion: a critical review. J Adhes Sci Technol 6:1269–1302

Guo J (2004) Recent progress in nanoimprint technology and its applications. J Phys D Appl Phys 37:R123–R141

Hess HF, Pettibone D, Adler D, Bertsche K, Nordquist KJ, Mancini DP, Dauksher J, Resnick DJ (2004) Inspection of templates for imprint lithography. J Vac Sci Technol B22:3300–3305

Hirai Y, Harada S, Isaka S, Kobayashi M, Tanaka Y (2002) Nanoimprint lithography using replicated mold by Ni electroforming. Jpn J Appl Phys 41:4186–4189

Hiroshima H, Komuro M (2007) UV-nanoimprint with the assistance of gas condensation at atmospheric environmental pressure. J Vac Sci Technol B 25:2333–2336

Hui CY, Jagota A, Lin YY, Kramer EJ (2002) Constraints on microcontact printing imposed by stamp deformation. Langmuir 18:1394–1407

Israelachvili JN (2011) Intermoleular and surface forces. Academic Press Elsevier, Amsterdam

Kim YS, Suh KY, Lee HH (2001) Fabrication of three-dimensional microstructures by soft molding. Appl Phys Lett 79:2285–2287

Kim K-D, Altun A, Choi D-G, Jeong J-H (2008) A 4-in-based single-step UV-NIL tool using a low vacuum environment and additional air pressure. Microelectr Eng 85:2304–2308

Landau LD, Lifschitz EM (2007) Hydrodynamik, vol VI. Harry Deutsch, Frankfurt

Merkel TC, Bondar VI, Nangai K, Freeman BD, Pinnau I (2000) Gas sorption, diffusion and permeation in poly(dimethylsiloxane). J Polym Sci B 38:415–434

Möllenbeck S, Bogdanski N, Wissen M, Scheer H-C, Zajadacz J, Zimmer K (2007) Multiple replication of three-dimensional structures with undercuts. J Vac Sci Technol B25:247–251

Mühlberger M, Bergmair I, Klukowska A, Kolander A, Leichtfried H, Platzgummer E, Loeschner H, Ebm C, Grützner G, Schöftner R (2009) UV-NIL with working stamps made from Ormostamp. Microelectron Eng 86:691–693

Odom TW, Love JC, Wolfe DB, Paul KE, Whitesides G (2002) Improved pattern transfer in soft lithography using composite stamps. Langmuir 18:5314–5320

Park S, Schift H, Solak HH, Gobrecht J (2004) Stamps for nanoimprint lithography by extreme ultraviolet interference lithography. J Vac Sci Technol B 22:3246–3250

Roos N, Wissen M, Glinsner T, Scheer H-C (2003) Impact of vacuum environment on the hot embosing process. SPIE Proc 5037:211–218

Roth CB, Dutcher JR (2005) Glass transition and chain mobility in thin polymer films. J Electroanal Chem 584:13–22

Scheer H-C, Schulz H (2001) A contribution to the flow behaviour of thin polymer films during hot embossing lithography. Microelectron Eng 56:311–332

Scheer H-C, Bogdanski N, Wissen M (2005) Issues in nanoimprint processes: the imprint pressure. Jpn J Appl Phys 44:5609–5616

Scheer H-C, Häfner W, Fiedler A, Möllenbeck S, Bogdanski N (2008) Quality assessment of antisticking layers for thermal nanoimprint. J Vac Sci Technol B26:2380–2384

Scheer H-C, Bogdanski N, Möllenbeck S, Mayer A (2009) Recovery prevention via pressure control in thermal nanoimprint lithography. J Vac Sci Technol B27:2882–2887

Scheer H-C, Mayer A, Dhima K, Wang S, Steinberg C (2013) Challenges with high aspect ratio nanoimprint. Microsyst Technol. doi:10.1007/s00542-013-1968-8

Schift H (2008) Nanoimprint lithography: an old story in modern times? A review. J Vac Sci Technol B26:458–480

Schift H, Saxer S, Park S, Padeste C, Pieles U, Gobrecht J (2005) Controlled co-evaporation of silanes for nanoimprint stamps. Nanotechnology 16:S171–S175

Schift H, Spreu C, Saidani M, Bednarzik M, Gobrecht J, Klukowska A, Reuther F, Gruetzner G, Solak H (2009) Transparent hybrid polymer stamp copies with sub-50-nm resolution for thermal and UV nanoimprint. J Vac Sci Technol B27:2846–2849

Schmid H, Michel B (2000) Siloxane polymers for high-resolution, high-accuracy soft lithography. Macromolecules 33:3042–3049

Sperling LH (2001) Introduction to physical polymer science. Wiley, Hoboken

Suh KY, Lee HH (2002a) Capillary force lithography: large-area patterning, self-organization and anisotropic dewetting. Adv Funct Mater 12:405–413

Suh KY, Lee HH (2002b) Self-organized polymeric microstructures. Adv Mater 14:346–351

Suh KY, Chu S, Lee HH (2004) W-shaped meniscus from thin polymer films in microchannels. J Micromech Microeng 14:1185–1189

Taga A, Yasuda M, Kawata H, Hirai Y (2010) Impact of molecular size on resist filling process in nanoimprint lithography: molecular dynamics study. J Vac Sci Technol B 28:C6M68–C6M71

Tsunozaki K, Kawaguchi Y (2009) Preparation methods and characteristics of fluorinated polymers for mold replication. Microelectron Eng 86:694–696

van Delft F, van de Laar R, Verschuuren M, Platzgummer E, Loeschner H (2010) Template masters for substrate conformal imprint lithography generated by charged particle nanopatterning techniques. Proc SPIE 7545:75450S1–75450S12

van Krevelen DW (1990) Properties of polymers. Elsevier, Amsterdam

Vratzov B, Fuchs A, Lemme M, Henschel W, Kurz H (2003) Large scale ultraviolet-based nanoimprint lithography. J Vac Sci Technol B 21:2760–2764

Xu F, Stacey N, Watts M, Truskett V, McMackin I, Choi J, Schumaker P, Thompson E, Babbs D, Sreenivasan SV, Willson G, Schumaker N (2004) Development of imprint materials for the step and flash imprint lithography process. Proc SPIE 5374:232–241

Yoo PJ, Choi S-J, Kim JH, Suh D, Baek SJ, Kim TW, Lee HH (2004) Unconventional patterning with a modulus-tunable mold: from imprinting to microcontact printing. Chem Mater 16:5000–5005

Young T (1805) An essay on the cohesion of fluids. Philos Trans R Soc Lond 95:65–87

Zhao Y, Berenschot E, de Broer M, Jansen H, Tas N, Huskens J, Elwenspoek M (2008) Fabrication of silicon oxide stamp for nanoimprint lithography by edge lithography reinforced with silicon nitride. J Micromech Microeng 18:064013 (6 pp)